PHYSICAL REVIEW APPLIED 3, 051002 (2015)

Ultrabroadband Midinfrared Pump-Probe Spectroscopy Using Chirped-Pulse Up-conversion in Gases

Hideto Shirai,[1,*] Tien-Tien Yeh,[2] Yutaka Nomura,[1] Chih-Wei Luo,[2] and Takao Fuji[1]

[1]*Institute for Molecular Science, 38 Nishigonaka, Myodaiji, Okazaki 444-8585, Japan*

[2]*Department of Electrophysics, National Chiao Tung University, Hsinchu 300, Taiwan*

(Received 6 January 2015; revised manuscript received 8 April 2015; published 28 May 2015)

We demonstrate ultrabroadband and ultrafast midinfrared (MIR) pump-probe spectroscopy by employing the chirped-pulse up-conversion technique with four-wave difference-frequency generation in a gas. The full spectra of the MIR probe pulses, which spread from 200 to 5000 cm^{-1}, are recorded on a single-shot basis. We apply this MIR pump-probe spectroscopy to measure the ultrafast carrier dynamics of an intrinsic germanium crystal wafer. Ultrafast reflectivity change induced by the excitation of carriers is observed in the region from far to near infrared. The behavior of the reflectivity-change signals at each delay time is explained by the Drude model.

DOI: 10.1103/PhysRevApplied.3.051002

I. INTRODUCTION

Midinfrared (MIR) light is crucially important for studies in molecular science and solid-state physics since a number of optical transitions have resonance energies in this frequency region. Pump-probe spectroscopy using ultrafast MIR pulses is a powerful tool for studying the ultrafast dynamics of photoexcited molecules and solid materials such as vibrational relaxation processes of liquid water [1–3], proton transfer and isomerization of protein [4,5], the behavior of Dirac fermions near the Dirac point of topological insulators [6], and phase transition and electron-hole transition of semiconductors [7–9].

A typical MIR coherent light source is based on optical parametric amplification. The bandwidth of the ultrashort pulses generated from such a light source is limited to $\sim$1000 cm^{-1} because of the phase-matching condition of the crystals for the parametric amplification [10]. The bandwidth is not usually broad enough for observing the high-reflection band caused by the free carriers, which can spread from the MIR to the terahertz region [11,12]. Moreover, even when narrow absorption lines such as those caused by lattice vibration are the interest in research, the high-reflection band caused by strong absorption is significantly broadened by the Kramers-Kronig relationship [13]. Therefore, an ultrabroadband light source extending to the MIR region as well as the terahertz region is desired and extremely important for investigating the detailed ultrafast dynamics in solids.

Recently, the generation of ultrabroadband MIR coherent light by using four-wave difference-frequency generation (FWDFG) of two-color femtosecond pulses in gases was demonstrated [14–16]. The use of gas media enables us to generate ultrabroadband MIR spectra spanning from 200 to 5500 cm^{-1}. The light sources developed with this technique have been successfully applied to advanced spectroscopy [17,18].

On the other hand, the measurement of such an ultrabroadband MIR spectrum is not a trivial task. While the Fourier-transform infrared spectrometer is capable of measuring such an ultrabroadband MIR spectrum, the acquisition speed is limited because it is necessary to scan the delay of the interferometer in the spectrometer. The combination of a multichannel mercury-cadmium-telluride array and a dispersive spectrometer would be capable of measuring MIR spectra without scanning the delay. However, in order to measure a spectrum spanning more than three octaves, it is necessary to exchange the grating and repeat the measurement to avoid the stray light from the high-order diffraction.

An alternative method to detect such an ultrabroadband MIR spectrum is optically converting the spectrum into the visible region through nonlinear effects and recording them with a visible spectrometer [19,20]. Nomura *et al.* reported single-shot measurements of ultrabroadband MIR spectra using chirped-pulse up-conversion (CPU) with gas media [21]. Thanks to the broadband phase matching of gas media, MIR spectra extending from 200 to 5500 cm^{-1} are measured.

In this Letter, we demonstrate ultrabroadband MIR pump-probe spectroscopy using CPU with gas media. An ultrabroadband MIR pulse generated through filamentation is used as a probe pulse, and the probe pulse reflected by a sample is up-converted to a visible-light pulse by using four-wave mixing in nitrogen gas. The spectrum of the probe pulse is recorded in a single shot by using a visible spectrometer. As a proof-of-principle experiment, we used our system to measure free-carrier dynamics of an intrinsic (100) germanium (Ge) crystal wafer. Ultrafast reflectivity

*shirai@ims.ac.jp

change, induced by photoinduced free carriers, is clearly observed in the region from 200 to 5000 cm^{-1}.

II. EXPERIMENT

The ultrabroadband MIR pump-probe spectroscopy with CPU in gas is realized with the system shown in Fig. 1. The light source is based on a Ti:sapphire multipass amplifier system (800 nm, 30 fs, 0.85 mJ at 1 kHz, Femtopower compactPro, FEMTOLASERS). The output pulse is split into three with two beam splitters. The first pulse is used for ultrabroadband MIR generation, the second pulse is used as the pump pulse for the pump-probe spectroscopy, and the third pulse is used for preparing a chirped pulse. The energies of the pulses are 510, 210, and 130 μJ, respectively.

The ultrabroadband MIR pulse (ω_0), which is used as the probe pulse, is generated by combining the fundamental (800 nm, ω_1) and second harmonic (SH, 400 nm, ω_2) pulses output from the Ti:sapphire amplifier by FWDFG ($\omega_1 + \omega_1 - \omega_2 \rightarrow \omega_0$) through filamentation in nitrogen. The pulse duration of the MIR pulse is 8.2 fs, which is confirmed with a cross-correlation frequency-resolved optical-gating measurement [15].

The generated MIR pulse is collimated by a concave mirror ($f = 0.25$ m) with a hole. Since the MIR pulse has a ring-shaped beam profile with the cone angle of ~3° [15,16,22], the use of the concave mirror with a hole is one of the most efficient ways to remove the residual visible beams (fundamental and SH) traveling along the MIR pulse. Additionally, the MIR pulse is reflected by three fused-silica substrates coated with indium tin oxide (ITO, $t = 300$ nm), which is transparent for visible light and reflects the MIR light effectively [23], to further reduce the residual visible beams. The MIR pulse is focused onto a sample by using a concave mirror ($f = 0.75$ m). The diameter of the MIR pulse on the sample is 0.4 mm. The pulse energy at the sample position is measured as 0.2 μJ by using a pyroelectric detector (J-10MB-LE, Coherent). From these values, the fluence of the MIR pulse at the sample is estimated as ~125 $\mu J/cm^2$.

The pump pulse (800 nm, 30 fs) is collimated down to the diameter of 4 mm with a combination of a concave mirror and a convex mirror, and overlapped with the MIR pulse on the sample. The angle between the pump pulse and the MIR pulse is ~3°. In this scheme, the relative delay between the pump pulse and the probe pulse varies with the transverse position on the sample. This effect reduces the time resolution to ~70 fs. For shot-to-shot data acquisition of reflectivity-change signals, every second pump pulse is blocked by using a mechanical chopper, which is synchronized with the half-frequency of the repetition rate of the laser pulse train.

The third beam is sent through four BK7 ($t = 10$ mm) substrates and a ZnSe ($t = 5$ mm) substrate at the Brewster angles. The transmitted pulse is chirped with the total group delay dispersion of ~6900 fs^2. The chirped pulse is combined with the MIR pulse using a mirror with a hole. The combined beam is focused into nitrogen with an off-axis parabolic mirror ($f_{eff} = 50$ mm) and up-converted into visible light (ω_2, 400–500 nm) through an FWDFG process ($\omega_1 + \omega_1 - \omega_0 \rightarrow \omega_2$) of the chirped pulse and the MIR pulse.

The up-converted spectrum is recorded with a spectrometer consisting of an imaging spectrograph and an electron-multiplying CCD camera (SP-2358 and ProEM + 1600, Princeton Instruments). The up-converted spectrum is obtained at each delay time between the pump and probe pulses by averaging 100 pairs of infrared spectra with or without pump to achieve a reasonable signal-to-noise ratio. The whole system is purged with nitrogen to reduce the absorption of carbon dioxide and water vapor.

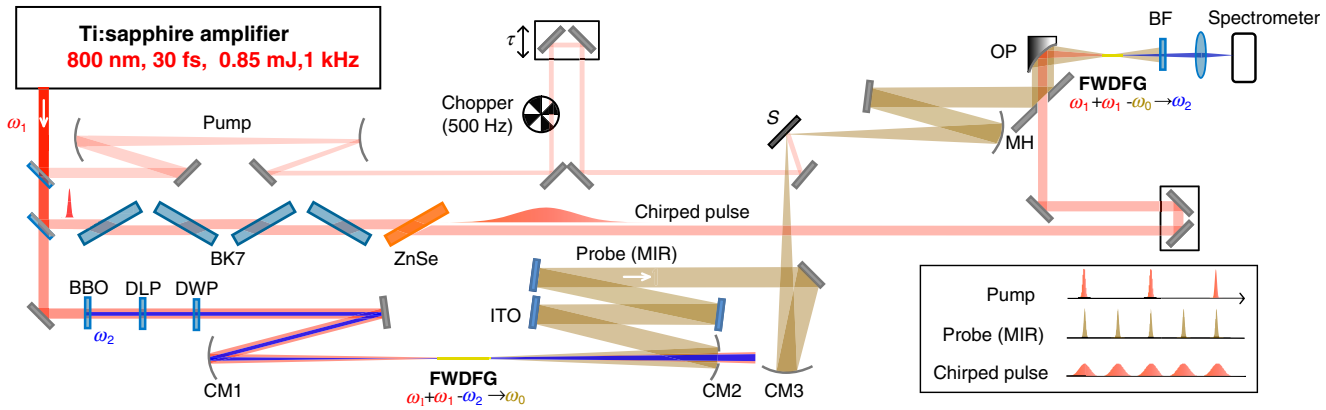

FIG. 1. Schematic illustration of ultrabroadband MIR pump-probe spectroscopy with chirped-pulse up-conversion in gas. BBO, β-BaB_2O_4; DLP, delay plate; DWP, dual-wave plate; ITO, indium-tin-oxide–coated plate; CM1, $r = 1$ m concave mirror; CM2, $r = 0.5$ m concave mirror with a hole ($\phi = 0.7$ mm); CM3, $r = 1.5$ m concave mirror; *S*, sample; MH, aluminum-coated mirror with a hole ($\phi = 7$ mm); OP, off-axis parabola ($f_{eff} = 50$ mm); BF, blue filter.

III. RESULT AND DISCUSSIONS

Figure 2(a) shows a typical spectrogram of the up-converted MIR pulse obtained by changing the delay between the chirped pulse and the MIR pulse. The frequency resolution of the CPU is proportional to the inverse of the pulse duration of the chirped pulse. The pulse duration of the chirped pulse is estimated as ∼0.4 ps from a cross-correlation curve obtained by integrating the spectrogram along the frequency axis [Fig. 2(b)]. The frequency resolution in this condition is estimated as ∼40 cm^{-1}, which is enough for resolving reflection spectra of free carriers. Although higher frequency resolution could be obtained by further stretching the chirped pulse, it would also decrease the signal level.

In general, the up-converted spectrum is distorted by cross-phase-modulation caused by the chirped pulse. The original MIR spectrum is retrieved from the distorted up-converted spectrum by using a Fourier-transform algorithm [24]. The algorithm requires an experimental value of the second-order spectral-phase parameter of the chirped pulse, which is obtained by measuring a spectrally resolved cross-correlation signal between the chirped pulse and the MIR pulse as a function of the delay time [20,21]. The dotted line in Fig. 2(a) shows the instantaneous frequency of the chirped pulse, which is obtained by fitting the instantaneous up-converted frequency of the absorption line of the carbon dioxide with a linear function. The second-order spectral-phase parameter of the chirped pulse is estimated as 3.26×10^3 fs^2.

A typical up-converted spectrum of the MIR pulse is shown as the upper curve in Fig. 3. The spectrum spreads from 400 to 510 nm. The up-converted spectrum could be obtained with the MIR pulse energy as low as 6 nJ in this experimental condition. The original MIR spectrum can be retrieved by flipping and shifting the up-converted spectrum [21]. The retrieved MIR spectrum is shown as the lower curve in Fig. 3. It is clear that the full spectrum of the ultrabroadband MIR pulse, which spreads from 200 to 5000 cm^{-1}, can be obtained with the CPU technique.

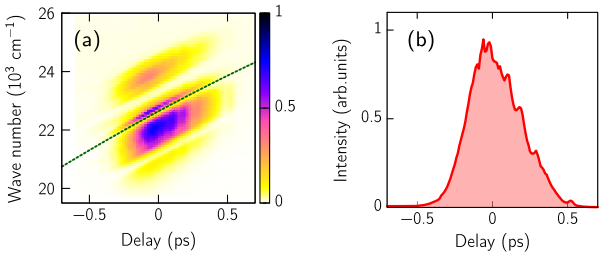

FIG. 2. (a) A typical spectrogram of the up-converted MIR pulse obtained by changing the delay between the chirped pulse and the MIR pulse. The dotted line is the instantaneous frequency obtained by fitting the absorption line of carbon dioxide. (b) The cross-correlation signal obtained by integrating the spectrogram along the frequency axis.

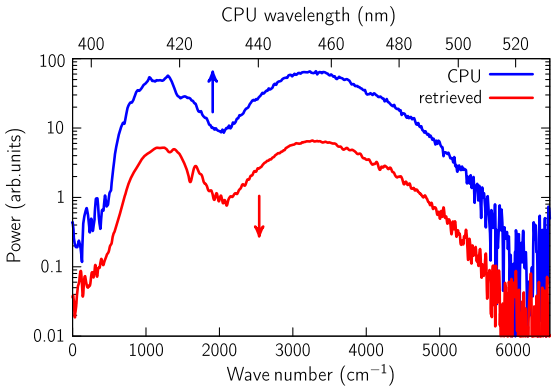

FIG. 3. A typical up-converted spectrum (upper curve) and the retrieved MIR spectrum (lower curve).

To test the performance of our CPU system, we measured MIR absorption spectra of water by using a setup similar to that in Ref. [25] and compared the result with spectra measured with a conventional FT-IR spectrometer (FT/IR-6100, JASCO). Those spectra agreed almost completely in this frequency region. This result indicates that the CPU system allowed us to measure the spectra accurately without nonlinear effects such as saturation in our experimental condition.

We apply the system to measure the transient reflectivity change of an intrinsic Ge crystal wafer with a thickness of 5 mm. Figure 4 shows the transient reflectivity-change signals $\Delta R/R$ of a Ge crystal wafer at the excitation fluence of 135 $\mu J/cm^2$. As a distinct feature, positive and negative reflectivity-change signals are clearly observed and the negative signal spreads to ∼5000 cm^{-1}. The use of ultrabroadband MIR probe pulses enabled us to obtain the entire spectrum of the transient reflectivity-change signals.

Such a reflectivity-change signal indicates a signature of metallic phase induced by photoinduced free carriers. The change in the complex permittivity of semiconductors caused by free carriers can be described by the Drude model [7]. The complex permittivity $\epsilon(\omega)$ is expressed as

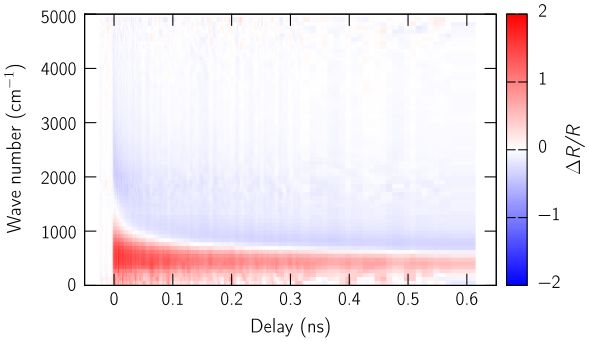

FIG. 4. Transient reflectivity-change signal $\Delta R/R$ of Ge under 135 $\mu J/cm^2$.

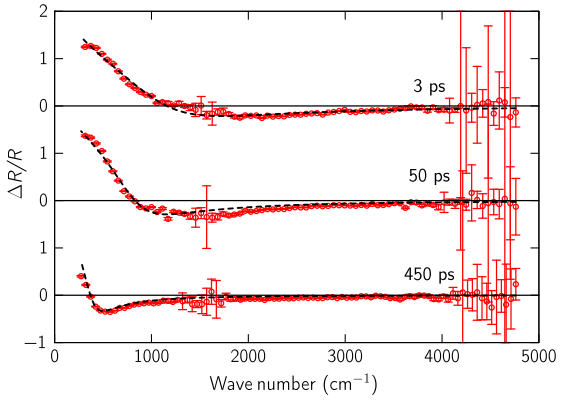

FIG. 5. Time-resolved reflectivity-change spectra $\Delta R/R$ at 3, 50, and 450 ps under 135 μJ/cm^2 excitation fluence. The circles are experimental results. The error bars are standard errors estimated by averaging over 100 spectra. The dashed lines are the fitting curves with the Drude model shown as Eq. (1)

$$\epsilon(\omega) = \epsilon_\infty\left(1 - \frac{\omega_P^2}{\omega^2 - i\omega\gamma}\right), \qquad (1)$$

where ϵ_∞ is the limiting value of the permittivity at high frequency, and γ is the carrier scattering rate. The plasma frequency ω_P is defined as $\omega_P = \sqrt{Ne^2/\epsilon_0\epsilon_\infty m^*}$, where N is the carrier concentration, ϵ_0 is the vacuum permittivity, and m^* denotes the electron effective mass. The measured reflectivity-change signals are fitted by using the plasma frequency and damping rate as the variable parameters. The Fresnel reflection at the same experimental condition is taken into account for the calculation. The MIR pulse is incident at an angle of 45° with p polarization. We assumed $m^* = 0.34m_e$ [26] and $\epsilon_\infty = 16$ [27]. Reference reflectance is set to 0.24, which corresponds to a condition where free carriers are not present in the Ge crystal wafer.

Figure 5 shows the reflectivity-change signals at different delay times under 135 μJ/cm^2 excitation fluence. The circles show the experimental data, whereas the error bars show standard errors estimated by averaging over 100 spectra. The standard errors around 1600 cm^{-1} are large because the up-converted spectrum around this wavelength region has relatively large fluctuation. The dashed curve shows the fitting curve obtained with the Drude model, which agrees well with the experimental data at each delay time. Therefore, we believe that the Drude model is suitable to explain the dynamics of the reflectivity change observed in this experiment.

In previous visible-light–pump and MIR-probe experiments, the bandwidths are narrow [9,28]. In contrast, the bandwidth of our probe pulse is so broad that the entire free-carrier behavior predicted by the Drude model could be experimentally visualized. Although such reflectivity-change spectra in a similar MIR range has been measured by using a synchrotron radiation source with 100 ps time resolution [26], our time resolution of 70 fs is several orders of magnitude higher.

IV. CONCLUSION

In conclusion, we demonstrate ultrabroadband MIR pump-probe spectroscopy using chirped-pulse up-conversion with FWDFG in a gas medium. The time resolution is 70 fs and the detection frequency range is from 200 to 5000 cm^{-1}. We succeed in measuring the transient reflectivity change caused by the photoinduced free carriers of an intrinsic Ge crystal wafer. The observed transient-reflectivity-change signals can be qualitatively explained by using the Drude model. The lowest MIR pulse energy for detecting the CPU spectra is as low as ~6 nJ in our experimental condition. This suggests that the up-conversion could be achieved with less expensive laser systems with lower pulse energies. We believe that the demonstrated pump-probe system based on chirped-pulse up-conversion is useful for the studies in solid-state physics and molecular science.

ACKNOWLEDGMENTS

This work was supported by JSPS KAKENHI (24360030, 15K17475), SENTAN JST (Japan Science and Technology Agency), the RIKEN-IMS joint Programme on "Extreme Photonics," and Consortium for Photon Science and Technology. T. T. Y. acknowledges the EXODASS program for expenses during her work in Japan.

[1] S. Woutersen, U. Emmerichs, and H. J. Bakker, Femtosecond mid-IR pump-probe spectroscopy of liquid water: Evidence for a two-component structure, Science **278**, 658 (1997).

[2] A. J. Lock and H. J. Bakker, Temperature dependence of vibrational relaxation in liquid H_2O, J. Phys. Chem. **117**, 1708 (2002).

[3] Han-Kwang Nienhuys, Sander Woutersen, Rutger A. van Santen, and Huib J. Bakker, Mechanism for vibrational relaxation in water investigated by femtosecond infrared spectroscopy, J. Phys. Chem. **111**, 1494 (1999).

[4] Jasper J. van Thor, Giulia Zanetti, Kate L. Ronayne, and Michael Towrie, Structural events in the photocycle of green fluorescent protein, J. Phys. Chem. B **109**, 16099 (2005).

[5] M. L. Groot, L. J. G. W. Van Wilderen, D. S. Larsen, M. A. Van der Horst, I. H. M. Van Stokkum, K. J. Hellingwerf, and R. Van Grondelle, Initial steps of signal generation in photoactive yellow protein revealed with femtosecond mid-infrared spectroscopy, Biochemistry **42**, 10054 (2003).

[6] C. W. Luo, H. J. Wang, S. A. Ku, H.-J. Chen, T. T. Yeh, J.-Y. Lin, K. H. Wu, J. Y. Juang, B. L. Young, T. Kobayashi, C.-M. Cheng, C.-H. Chen, K.-D. Tsuei, R. Sankar, F. C. Chou, K. A. Kokh, O. E. Tereshchenko, E. V. Chulkov, Yu. M. Andreev, and G. D. Gu, Snapshots of dirac fermions near

the dirac point in topological insulators, Nano Lett. **13**, 5797 (2013).

[7] M. Nagai, R. Shimano, and M. Kuwata-Gonokami, Electron-Hole Droplet Formation in Direct-Gap Semiconductors Observed by Mid-Infrared Pump-Probe Spectroscopy, Phys. Rev. Lett. **86**, 5795 (2001).

[8] M. Nagai and M. Kuwata-Gonokami, Time-resolved reflection spectroscopy of the spatiotemporal dynamics of excited carriers in Si and GaAs, J. Phys. Soc. Jpn. **71**, 2276 (2002).

[9] J. Zhu, T. Mathes, A. D. Stahl, J. T. M. Kennis, and M. L. Groot, Ultrafast mid-infrared spectroscopy by chirped pulse upconversion in 1800–1000 cm^{-1} region, Opt. Express **20**, 10562 (2012).

[10] B. W. Mayer, C. R. Phillips, L. Gallmann, M. M. Fejer, and U. Keller, Sub-four-cycle laser pulses directly from a high-repetition-rate optical parametric chirped-pulse amplifier at 3.4 μm, Opt. Lett. **38**, 4265 (2013).

[11] F. Ganikhanov, K. C. Burr, D. J. Hilton, and C. L. Tang, Femtosecond optical-pulse-induced absorption and refractive-index changes in GaAs in the midinfrared, Phys. Rev. B **60**, 8890 (1999).

[12] T. Inushima, M. Higashiwaki, and T. Matsui, Optical properties of Si-doped InN grown on sapphire (0001), Phys. Rev. B **68**, 235204 (2003).

[13] Charles Kittel, *Introduction to Solid State Physics*, 6th ed. (John Wiley & Sons, Inc., New York, 1986).

[14] T. Fuji and T. Suzuki, Generation of sub-two-cycle mid-infrared pulses by four-wave mixing through filamentation in air, Opt. Lett. **32**, 3330 (2007).

[15] Y. Nomura, H. Shirai, K. Ishii, N. Tsurumachi, A. A. Voronin, A. M. Zheltikov, and T. Fuji, Phase-stable sub-cycle mid-infrared conical emission from filamentation in gases, Opt. Express **20**, 24741 (2012).

[16] T. Fuji and Y. Nomura, Generation of phase-stable sub-cycle mid-infrared pulses from filamentation in nitrogen, Appl. Sci. **3**, 122 (2013).

[17] C. Calabrese, A. M. Stingel, L. Shen, and P. B. Petersen, Ultrafast continuum mid-infrared spectroscopy: Probing the entire vibrational spectrum in a single laser shot with femtosecond time resolution, Opt. Lett. **37**, 2265 (2012).

[18] A. M. Stingel, C. Calabrese, and P. B. Petersen, Strong intermolecular vibrational coupling through cyclic hydrogen-bonded structures revealed by ultrafast continuum mid-IR spectroscopy, J. Phys. Chem. B **117**, 15714 (2013).

[19] E. J. Heilweil, Ultrashort-pulse multichannel infrared spectroscopy using broadband frequency conversion in $LiIO_3$, Opt. Lett. **14**, 551 (1989).

[20] C. R. Baiz and K. J. Kubarych, Ultrabroadband detection of a mid-IR continuum by chirped-pulse upconversion, Opt. Lett. **36**, 187 (2011).

[21] Y. Nomura, Y.-T. Wang, T. Kozai, H. Shirai, A. Yabushita, C.-W. Luo, S. Nakanishi, and T. Fuji, Single-shot detection of mid-infrared spectra by chirped-pulse upconversion with four-wave difference frequency generation in gases, Opt. Express **21**, 18249 (2013).

[22] Alexander A. Voronin, Yutaka Nomura, Hideto Shirai, Takao Fuji, and Aleksei Zheltikov, Half-cycle pulses in the mid-infrared from a two-color laser-induced filament, Appl. Phys. B **117**, 611 (2014).

[23] Scott H. Brewer and Stefan Franzen, Optical properties of indium tin oxide and fluorine-doped tin oxide surfaces: Correlation of reflectivity, skin depth, and plasmon frequency with conductivity, J. Alloys Compd. **338**, 73 (2002).

[24] K. F. Lee, P. Nuernberger, A. Bonvalet, and M. Joffre, Removing cross-phase modulation from midinfrared chirped-pulse upconversion spectra, Opt. Express **17**, 18738 (2009).

[25] H. Shirai, C. Duchesne, Y. Furutani, and T. Fuji, Attenuated total reflectance spectroscopy with chirped-pulse upconversion, Opt. Express **22**, 29611 (2014).

[26] Lee Carroll, Peter Friedli, Philippe Lerch, Jörg Schneider, Daniel Treyer, Stephan Hunziker, Stefan Stutz, and Hans Sigg, Ultra-broadband infrared pump-probe spectroscopy using synchrotron radiation and a tuneable pump, Rev. Sci. Instrum. **82**, 063101 (2011).

[27] M. I. Gallant and H. M. van Driel, Infrared reflectivity probing of thermal and spatial properties of laser-generated carriers in germanium, Phys. Rev. B **26**, 2133 (1982).

[28] J. Knorr, P. Rudolf, and P. Nuernberger, A comparative study on chirped-pulse upconversion and direct multichannel MCT detection, Opt. Express **21**, 30693 (2013).